TABLE II. Calculated and measured positions for the spacings observed in KCN IV assuming a rhombohedral lattice. Only those peaks which could be resolved are listed. Lattice parameters $a_{hex} = 5.1906 \pm 0.0007$ Å, $c_{hex} = 6.9129 \pm 0.0023$ Å, $a_{rh} = 3.780$, and $\alpha_{rh} = 86°42'$. Volume of rhombohedral unit cell = 53.77 ± 0.03 Å^3.

hexagonal indexing	Rhombohedral indexing	d_{calc} (Å)	d_{obs} (Å)
101	100	3.7685	3.783 ± 0.002
012	110	2.7400	2.7405 ± 0.0011
110	$10\bar{1}$	2.5953	2.5954 ± 0.0004
003	111	2.3043	...
021	$11\bar{1}$	2.1375	2.1363 ± 0.0069
202	200	1.8842	1.8909 ± 0.0006
113	210	1.7231	1.7291 ± 0.0020
211	$20\bar{1}$	1.6500	1.6502 ± 0.0007
122	$21\bar{1}$	1.5248	1.5250 ± 0.0007
300	$2\bar{1}\bar{1}$	1.4984	1.4981 ± 0.0005
015	221	1.3215	1.3210 ± 0.0007
220	$20\bar{2}$	1.2976	1.2980 ± 0.0009

for well-known cubic materials, the measured $I_0(\lambda)$ was adjusted for the longer neutron wavelengths by dividing it by $[1+(\lambda-1.8)]^{1/2}$ for $\lambda > 1.8$ Å and by unity for $\lambda \leq 1.8$ before using it in Eq. (2) to calculate relative structure factors. We are not sure why this empirical correction is necessary, but different detector efficiencies could account for it.

In further analyzing the data for KCN IV, we modified the least-squares-fitting technique summarized in Eq. (1) in order to test particular space groups. In this case the term $\alpha_{\vec{h}}$ for the amplitude of the KCN peak with label $\vec{h}$ is replaced by the expression

$$\alpha_{\vec{h}} \rightarrow [\mu \lambda_i^4 I_0(\lambda_i)/S_i]\, m_{\vec{h}} |F_{\vec{h}}|^2 , \qquad (3)$$

where μ is an over-all intensity scaling factor for KCN and the relative intensities for the peaks are no longer arbitrary but fixed by the chosen space group. This analysis was particularly useful in refining the KCN IV structure since the KCN IV diffraction pattern contained overlapping peaks.

Since the intensity measurements are important to our interpretation of the diffraction patterns for the high-pressure phases we measured the intensities for the KCN I pattern at room temperature (see Table III) and compared them with the powder diffraction results in the literature.[7,17,18] These measurements were taken with the sample inside the pressure cell before application of pressure. We have scaled the results so that the TOF value for the intensity ($|F|^2$) of the (200) diffraction peak agrees with the literature value.[7,17,18] The good agreement with intensities obtained in previous powder neutron-diffraction studies confirms the accuracy of our spectrum determination and the validity of the empirical correction discussed earlier.

For the KCN III pattern (Fig. 2) the diffraction peaks were well resolved and the peaks could be analyzed separately using Eq. (1) to determine the best value for the intensity of each peak. For the (110) diffraction peak there appear to be some small intensity "wings" above the background which may be due to thermal diffuse scattering, but no explicit allowance was made for this in the intensity analysis. The relative structure factors $|F_{\vec{h}}|^2$ computed according to Eq. (2) were analyzed with a refinement program[19] to determine the position of the CN^- ion in the unit cell and the Debye-Waller factors for the K^+ and CN^- ions. Scattering lengths of $b_K = 0.37$, $b_C = 0.665$, and $b_N = 0.94$ in units of 10^{-12} cm per atom were assumed for the respective nuclei.[20]

Two different models were tried in the effort to determine the nature of the disordering among the linear CN^- molecules within the cubes formed by the K^+ ions in KCN III. Following Richter and Pistorius[6] we first tried the space group $Pm3m(O_h^1)$ in which the K^+ ions were placed at the origin and the C and the N atoms were averaged over the eight equivalent (g) positions at x_1, x_1, x_1 along the [111] directions in the cubic unit cell. The eight CN scattering centers were each assigned a scattering length of $\frac{1}{8}(b_C + b_N)$. The midpoint of the CN bond was fixed at $(\frac{1}{2}, \frac{1}{2}, \frac{1}{2})$. In the refinement calculation[19] the thermal factors B_K, B_{CN} are given by the quantity $\exp[-B(h^2+k^2+l^2)/4a^2]$ in the expression for the structure amplitude where a is the lattice parameter for KCN III. The results of the refinement fitting are given in Table I. The position of the CN group resulting from the refinement was $x_1 = 0.4071 \pm 0.0017$ yielding a C-N bond length of 1.23 ± 0.02 Å along one of the [111] directions. The thermal factors $B_K = 2.6 \pm 0.6$ Å^2 and $B_{CN} = 3.9 \pm 0.8$ Å^2 are quite large, reflecting the large amount of molecular libration present in this disordered system. Using the relation

$$B_{K,CN} = 8\pi^2 \langle \mu_x^2 \rangle_{K,CN} , \qquad (4)$$

the linear motional amplitude $\langle \mu_x^2 \rangle^{1/2}$ is 0.18 and 0.23 Å for the K^+ and CN^- ions, respectively. The R value for the first ten peaks, of which only seven are clearly visible above the background was 4.1%. The large thermal factors reduced the amplitude of the peaks associated with smaller lattice spacings below the statistical fluctuation in the background.

Next we tried a "free-rotation" model[17] in which

the K^+ ions were again fixed at the origin and the CN group was treated as a single entity which moved freely on the surface of a sphere whose center was at $(\frac{1}{2}, \frac{1}{2}, \frac{1}{2})$ and whose radius was one-half the CN bond length. The best fit resulted for bond lengths in the range 1.20~1.24 Å. The results for the fit with a bond length of 1.2 Å are tabulated in Table I. The R value for this fit was $R = 11.5\%$ which is to be compared with $R = 4.1\%$ for the fit to $Pm3m(O_h^1)$. The "free-rotation" model appears to be a much less satisfactory model for KCN III.

IV. ANALYSIS OF THE KCN IV PATTERN

The rhombohedral analysis of the KCN IV data exposed two serious problems. First, several of the diffraction peaks were broadened in excess of the instrumental broadening with shapes that were not truly Gaussian, so that the fitting program summarized in Eq. (1) could not be used to compare intensities. Second, although the observed diffraction peak positions for KCN IV given in Table II were very nearly consistent with a rhombohedral lattice with unit-cell constants $a_{rh} = 3.780$ Å, $\alpha_{rh} = 86.7°$, the (100), (200), and (210) diffraction peaks were displaced from their rhombohedral positions by more than the experimental uncertainty.

On the basis of high-pressure x-ray measurements, Pistorius[5] concluded that the most likely space group for KCN IV was $R\bar{3}m(D_{3d}^5)$. Here the K^+ ion is at (0, 0, 0) and the cyanide ion lies along the [111] rhombohedral axis but without distinction between the heads and tails of the CN^-'s. Using the modification of our fitting program summarized in Eq. (3) we tested this model. The CN^- group was treated as a single entity with a scattering length $b_{CN} = \frac{1}{2}(b_C + b_N)$. This "CN atom" was placed at $\pm(0, 0, z)$ in the hexagonal cell in which the c axis coincides with the [111] axis of the rhombohedral cell. The K^+ ion was placed at the origin as before. The expression for the structure amplitude in Eq. (3) becomes

$$F_{\vec{h}} = (b_K e^{-B_K/4d_{\vec{h}}^2} + b_{CN} e^{-B_{CN}/4d_{\vec{h}}^2} \times 2\cos 2\pi lz) \times \{1 + 2\cos[\tfrac{2}{3}\pi/(-h+k+l)]\}. \quad (5)$$

The fitting yielded a value for z of 0.4037 ± 0.0012, implying a CN bond length of 1.33 ± 0.02 Å. The results for the temperature factors for the K^+ ions and the CN^- group were, respectively, $B_K = 1.7 \pm 0.4$ Å^2, $B_{CN} = 5.0 \pm 0.3$ Å^2. The solid line in Fig. 3 represents the best fit of the KCN IV diffraction pattern to $R3m(D_{3d}^5)$. The poor intensity agreement apparent from the figure is reflected in the rather large goodness-of-fit value, 8.93 (See Sec. III). The displacement of the (100) and (200) diffraction peaks from their exact rhombohedral positions and the apparent line broadening for several of the diffraction peaks [(100), (110), and (200)] which was apparent in the fitting procedure summarized by Eq. (1) (no constraints on intensities) is also evident in Fig. 3. The errors given are statistical and do not reflect these problems in the fitting.

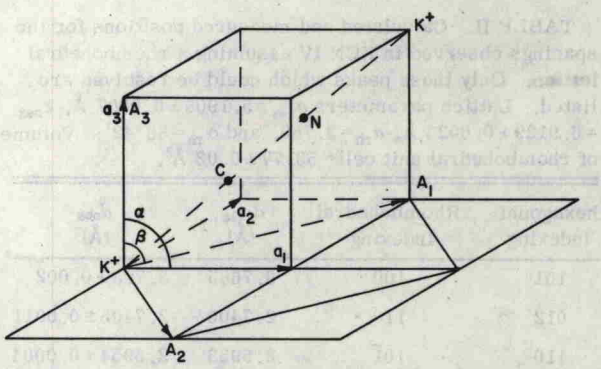

FIG. 4. Relation of the crystallographic unit cells for KCN III and KCN IV. $\vec{a}_1$, $\vec{a}_2$, $\vec{a}_3$ are the edges of the cubic cell for KCN III. $\vec{A}_1$, $\vec{A}_2$, and $\vec{A}_3$ are the edges of the C-centered monoclinic cell derived from the rhombohedral cell which results from the application of a small rhombohedral distortion to the cubic cell. The monoclinic cell for KCN IV may be pictured as the result of a rhombohedral distortion followed by a monoclinic distortion as described in the text. The C and N atoms, shown as lying along a [111] axis in the above figure, lie in ordered positions in the A_1A_3 plane in the monoclinic cell of KCN IV.

The diffraction peak broadening discussed above could arise either from a domain size effect[21] based on a short-range ordering of the CN^- molecule or from a distortion of the rhombohedral lattice to lower symmetry. The displacement of the (100) and (200) peaks from their positions in the rhombohedral lattice constitutes a strong argument for the latter explanation.

Since these displacements are small, the distortion from the rhombohedral structure must be small. The rhombohedral cell constants indicate only a slight distortion from the cubic structure of KCN III, and it is therefore convenient to start from the model sketched in Fig. 4 where $\vec{a}_1$, $\vec{a}_2$, and $\vec{a}_3$, ($a = 3.808$ Å) form the edges of the cubic cell. Here the C and N atoms are placed along a threefold [111] axis in the cubic cell consistent with the fact that the space group $R\bar{3}m(D_{3d}^5)$ with the cyanide ions lying along the rhombohedral axis enables a reasonably good description of the observed intensities (Fig. 3). The $R\bar{3}m(D_{3d}^5)$ space group can be generated by increasing the length of the cube diagonal so that the angle α is smaller than 90° ($\alpha = 86.7°$). This is accompanied by a decrease of a to 3.780 Å to agree with the rhombohedral lattice parameter. The vectors $\vec{a}_1$, $\vec{a}_2$, and $\vec{a}_3$ now become the basis vectors of the rhombohedral cell. We can describe this structure in terms of a monoclinic cell with